Quart. J. R. Met. Soc. (1980), **106**, pp. 707–719

551.511.32

The diagnosis of middle latitude synoptic development

By B. J. HOSKINS and M. A. PEDDER

UK Universities' Atmospheric Modelling Group and Department of Meteorology, University of Reading, Reading, UK

(Received 21 February 1980; revised 2 April 1980)

SUMMARY

The use of diagnostics based on different forms for the forcing term in the omega equation is explored. These forms are the two-level and continuous versions of the approximation used by Sutcliffe (1947) in his development theory, the usual dynamical meteorology version involving vorticity and thermal advection, and that involving the so-called Q-vectors which was introduced by Hoskins *et al.* (1978). The diagnostics are applied to a model baroclinic wave and to a subjectively analysed real data case. The Sutcliffe form is simplest and gives a global view of the system movement and development, but details such as active frontal regions are missed. The vorticity and thermal advection form has few advantages. It is demonstrated that the Q-vector analysis can provide more information than the Sutcliffe form in describing details of system development, particularly with respect to (a) a vectorial view of the horizontal ageostrophic motion field, and (b) some indication of the intensity of frontal circulations. A case is presented for including Q-vector fields in low- and mid-tropospheric forecast charts.

1. INTRODUCTION

The purpose of this paper is to further explore the use of diagnostics which were discussed in Hoskins *et al.* (1978, hereafter denoted Ω). There various forms of the forcing term F in the quasi-geostrophic 'omega equation'

$$N^2\nabla_h^2 w + f^2\frac{\partial^2 w}{\partial z^2} = F \qquad . \qquad . \qquad . \qquad (1)$$

were considered, N being the buoyancy frequency and f the Coriolis parameter. Before recalling these forms we first note that if w is approximately sinusoidal in the three space dimensions then F negative is expected to give w positive, i.e. upward motion.

Neglecting the variation of f with latitude and diabatic effects, the form of F given the name 'Sutcliffe' in Ω is

$$F_s = 2f\frac{\partial \mathbf{v}_g}{\partial z}.\nabla_h\zeta_g, \qquad . \qquad . \qquad . \qquad . \qquad (2)$$

where ξ_g is the vertical component of geostrophic relative vorticity.

Using a two-level representation with $\mathbf{v}_g = \mathbf{v}_0$ at $z = 0$ and $\mathbf{v}_g = \mathbf{v}_0 + \mathbf{v}'$ at $z = H$,

$$\begin{aligned} F_s &= 2(f/H)\mathbf{v}'.\nabla_h[\tfrac{1}{2}\{\xi_0 + (\xi_0 + \xi')\}] \\ &= (f/H)(2\mathbf{v}'.\nabla_h\xi_0 + \mathbf{v}'.\nabla_h\xi'). \qquad . \qquad . \qquad . \qquad (3) \end{aligned}$$

This is the form for F_s actually introduced by Sutcliffe (1947) in his development theory. Further analysis of this theory is given in Appendix A.

In Ω it was shown that the Sutcliffe form F_s, though convenient, neglects a term which formally is of the same order as those retained. The neglected term is proportional to the square of the deformation times the rotation of the dilatation axis with height and may be important in frontal regions and in jet entrance and exit regions. The usual form of the omega equation used by dynamical meteorologists makes no such approximation in writing

$$F_{VT} = f\frac{\partial}{\partial z}(\mathbf{v}_g.\nabla_h\zeta_g) - \frac{g}{\theta_0}\nabla_h^2(\mathbf{v}_g.\nabla_h\theta) \qquad . \qquad . \qquad (4)$$

where θ is potential temperature and θ_0 a reference value. This form, however, suffers from the tendency for the two terms to cancel and from the fact that the two terms individually are not Galilean invariant, i.e. independent of the translation of the coordinate axes. Thus an observer moving with velocity **U** would find an increase in the vorticity advection term by $f\mathbf{U}.\nabla(\partial\xi_g/\partial z)$ and a decrease in the thermal advection term by the same amount. This implies that physical understanding of the mechanisms for forcing vertical velocity achieved through this form is illusory. The relative advantages of the forms F_{VT} and F_s were also discussed by Trenberth (1978).

An alternative form for F which retains all quasi-geostrophic terms but does not have the problems of F_{VT} was presented in **Ω**. This form depended on defining a vector **Q** equal to the rate of change of potential temperature gradient moving with the horizontal geostrophic velocity

$$\mathbf{Q} = \frac{D_g}{Dt}\nabla_h\theta = \left[-\frac{\partial u_g}{\partial x}\frac{\partial\theta}{\partial x}-\frac{\partial v_g}{\partial x}\frac{\partial\theta}{\partial y}, \quad -\frac{\partial u_g}{\partial y}\frac{\partial\theta}{\partial x}-\frac{\partial v_g}{\partial y}\frac{\partial\theta}{\partial y}\right]. \qquad (5)$$

From this definition it is clear that the geostrophic frontogenesis function, i.e. the rate of change moving with the geostrophic motion of $|\nabla\theta|^2$ due to the geostrophic motion, is related to **Q** by

$$\left(\frac{\partial}{\partial t}+\mathbf{v}_g.\nabla\right)|\nabla_h\theta|^2 = 2\mathbf{Q}.\nabla_h\theta. \qquad (6)$$

The corresponding form for F is

$$F_Q = 2(g/\theta_0)\nabla_h.\mathbf{Q}. \qquad (7)$$

Put simply, where **Q** is convergent one expects upward motion and where it is divergent downward motion is implied. Following the analysis in **Ω**, if x' is a coordinate in the direction of the unit vector $\hat{\mathbf{i}}$ and u'_a the component of ageostrophic motion in that direction, then

$$N^2\frac{\partial w}{\partial x'}-f^2\frac{\partial u'_a}{\partial z} = 2(g/\theta_0)\mathbf{Q}.\hat{\mathbf{i}}. \qquad (8)$$

Thus the component of **Q** in any direction gives a measure of the circulation in a vertical section in that direction. The sense of the circulation is with **Q** pointing in the direction of

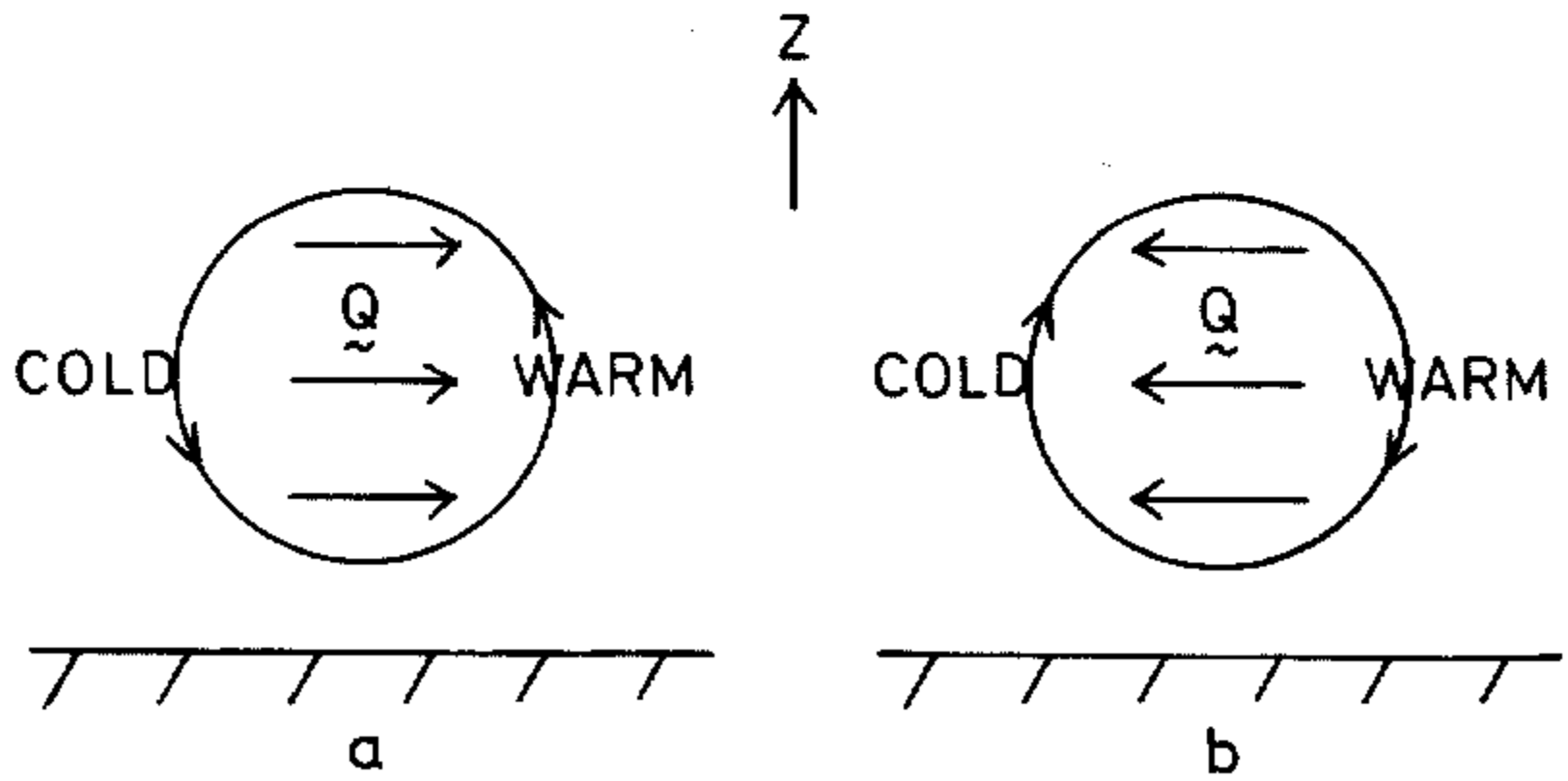

Figure 1. Diagrams showing two-dimensional frontogenetic (a) and frontolytic (b) situations. In (a) the large-scale geostrophic fields are tending to intensify the temperature gradient so that **Q** is in the direction from cold to warm air. The corresponding cross-frontal circulation is direct with the warm air rising and low-level ageostrophic flow towards the warm side. In (b) the large scale geostrophic fields are tending to weaken the temperature gradient, **Q** is reversed and so is the direction of the cross-frontal circulation.

the low-level ageostrophic motion and towards rising motion. Two-dimensional frontogenetic and frontolytic situations are illustrated in Fig. 1. Some further information on the meaning of Q-vectors is given in Appendix B and pressure coordinate versions of the equations used here are presented in Appendix C.

For comparison it is interesting to note that the other forms for F can also be written in the divergence form of Eq. (7). For the approximate Sutcliffe form given in Eq. (2) the vector $\mathbf{Q}$ is defined as

$$\mathbf{Q}_S = (f\xi\theta_0/g)(\partial \mathbf{v}_g/\partial z). \quad . \quad . \quad . \quad (9)$$

$\mathbf{Q}_S$ is not an approximation to $\mathbf{Q}$ and, unlike $\mathbf{Q}$, is always oriented along temperature contours at any level. For the vorticity and thermal advection form of Eq. (4) one may define

$$\mathbf{Q}_V = \frac{f\theta_0}{g}\frac{\partial}{\partial z}(\mathbf{v}_g\xi) \quad \text{and} \quad \mathbf{Q}_T = \nabla_h(\mathbf{v}_g \cdot \nabla_h\theta).$$

In this paper we shall investigate the use of these diagnostics using data from a theoretical model and from a real situation. The theoretical model of a growing baroclinic wave, which has been discussed in detail in Hoskins and West (1979) and Hoskins and Heckley (1980), provides in section 2 a comparison of the diagnostics with the actual model vertical velocities and predicted development. The real data case was diagnosed subjectively in Ω but here data reduction and analysis described in section 3 allow the quantitative diagnosis given in section 4.

2. Diagnosis of a theoretical model

The case for which diagnoses will be presented is for an initial zonal flow which is zero at the surface rising to a jet of the form $\cos^2 y$ at a lid (denoted by $\mu = 1$ in Hoskins and West (1979) and Hoskins and Heckley (1980)). Using the semi-geostrophic equations which are similar to the quasi-geostrophic equations but should remain valid in strong frontal situations, the development of a baroclinic wave to finite amplitude has been simulated. By day $5\frac{1}{2}$ the wave shows signs of the low-level vorticity maximum and strong temperature gradients consistent with a strong cold front. By day 6·3 (Fig. 2a) the surface cold front is very strong and a weaker warm front is pushing out east and south-east of the low. In the cited papers the frontogenesis has been studied and also the low- and mid-level vertical velocities have been exhibited. Consistent with the semi-geostrophic equations these vertical velocities have been obtained from an omega equation identical with Eq. (1) except that it is solved in a slightly distorted domain.

The diagnostics to be presented here are at the level $z = 2{\cdot}81$ km, $p = 743$ mb. In Fig. 2b is shown the temperature and $\mathbf{Q}$ fields and in Fig. 2c the model vertical velocity and $\mathbf{Q}$ fields all at this level. The Q-vectors dramatically depict the sinking in the cold air, the cross-frontal circulation in the cold front region and the rising in the warm air ahead of the system with, to a lesser extent, a warm-frontal circulation. The low-level vertical velocity field shown in Hoskins and Heckley (1980) further emphasizes these features. Recalling that the frontogenesis function is $\mathbf{Q}.\nabla_h\theta$ (Eq. (6)), the vectors shown in Fig. 2b display graphically the frontogenetic regions where potential temperature gradients are being enhanced. Thus the Q-vectors at this level as shown in Fig. 2b give a very reliable picture of the ageostrophic motions in the system and of its development.

For comparison we show in Fig. 2d the $\mathbf{Q}_S$ field consistent with the Sutcliffe form (Eq. (9)) and the vertical velocities implied by this approximation. The large-scale ascent and descent are captured, but the frontal circulations especially the rising ahead of and in

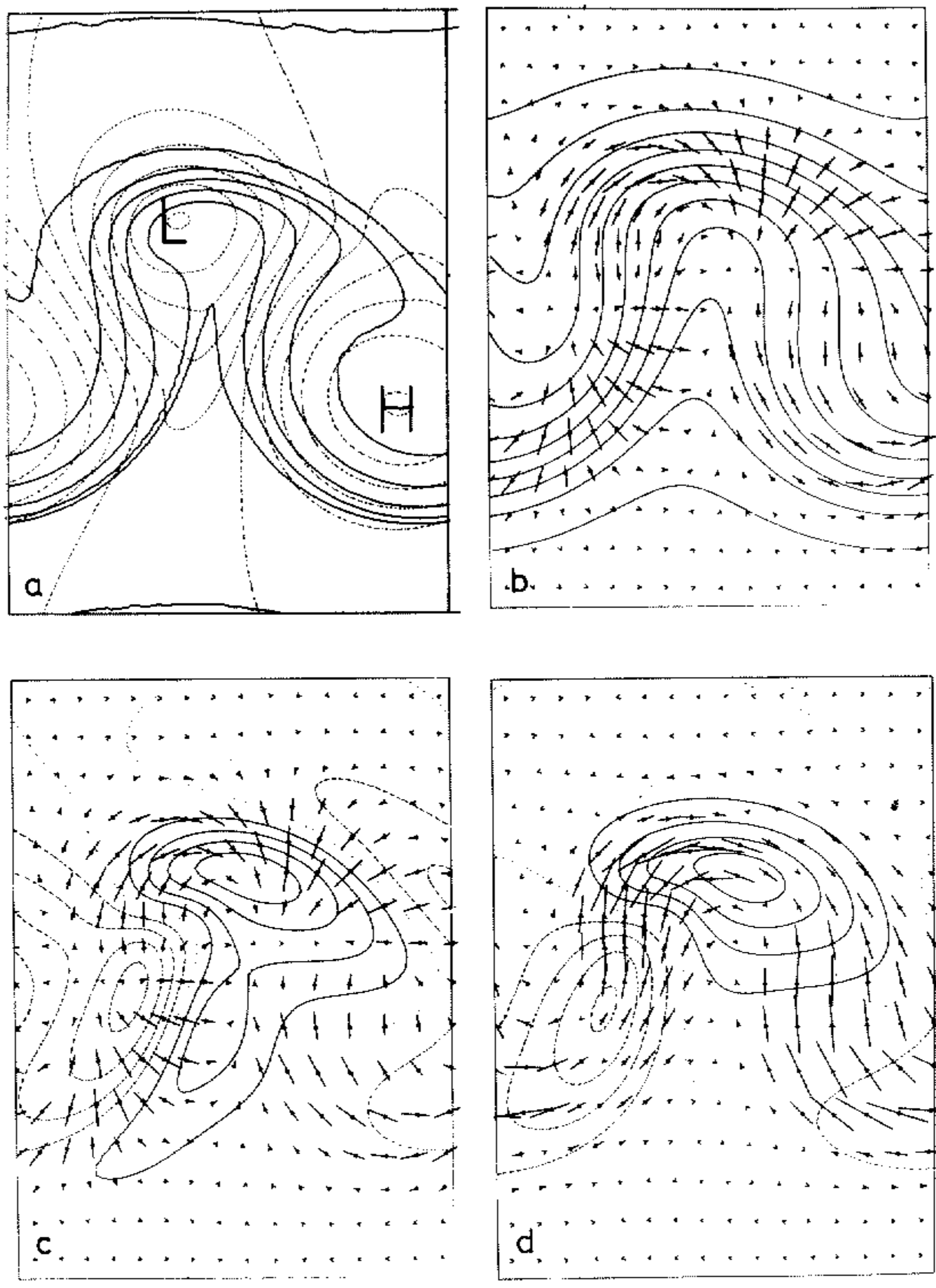

Figure 2. Maps illustrating the model baroclinic wave at day 6·3.
(a) Surface potential temperature and pressure. The potential temperature contour increment is 4 K and that for pressure is 6 mb.
(b) 2·81 km-level potential temperature and Q-vectors. The potential temperature contour increment is 4 K. The length scale for the Q-vector is such that the indicated latitudinal distance between grid rows corresponds to approximately $0{\cdot}5 \times 10^{-9}$ K m^{-1} s^{-1}.
(c) 2·81 km-level vertical velocity and Q-vectors. The contours of vertical velocity are drawn every 0·5 cm s^{-1} with positive contours being continuous, zero contours dotted and negative dashed.
(d) As (c) but using Sutcliffe approximations, Eqs. (2) and (9).

the cold-front region are absent. Further, the plotted vectors are not particularly helpful in visualizing details of the development.

3. Real case – data reduction and analysis

The real data case chosen was for 10 November 1975. During that day a major storm

developed over the mid-west of North America. Data for the estimation of the quasi-geostrophic forcing fields were extracted from subjectively analysed 700 mb and 500 mb surface pressure maps based on routine standard level upper air reports. On both maps, geopotential height contours were constructed following traditional synoptic guidelines, contour direction being constrained to be locally parallel to the reported wind direction, and contour spacing being adjusted to be near-geostrophically consistent with the reported wind speed, in both cases some tolerance being allowed in consideration of probable observing error limits or suspect observations. Contours of 1000 to 500 mb geopotential thickness were analysed after extensive gridding of the 500 mb height map over the corresponding surface mean-sea-level pressure and temperature analysis. The temperature field at 700 mb was analysed directly from reported temperatures at that level, with some consideration being given to the direction of surface isotherms in data-sparse areas of the chart.

Height, thickness and temperature values were interpolated subjectively from these charts onto a rectangular 15×17 point grid with spacing equivalent to 180 km at 40°N. Grid-point height and thickness values were estimated to the nearest 5 gpm, and 700 mb temperatures to the nearest 0·5°C, the latter being equivalent to a rounding error of the order of 10 gpm on 1000 to 500 mb thickness if 700 mb temperature is considered as being representative of mean 1000 to 500 mb temperature. A simple first order moving average filter was then applied to these fields in order to remove some of the spurious small-scale structure associated with rounding and interpolation errors.

A straightforward second order centred differencing scheme was applied to the filtered grid point data in order to calculate the various forcing terms and vector fields represented in Equations (2), (3), (4), (5), (7) and (9). Variations of f, $\partial f/\partial y$ and map scale within the analysis region were not taken into account, the errors associated with neglecting these terms being considered negligible compared with the probable margin of error associated with uncertainties in the original map analysis and subjective interpolation. Isopleths were drawn manually to represent the grid-point output values of the scalar forcing field variables within the central 9×11 grid-point domain.

Before comparing the results from this real case study with model results, it is relevant to note the following points concerning the chart analysis and 'real case' computations.

(i) The real case analysis was completed before any model simulations. Despite some subjectivity involved in data preparation and analysis of output fields, we thus consider that the real case analysis is free from any bias.

(ii) Taking into account the spatial density of observations, as well as the numerical filtering and differencing suggests that the real case analysis should be capable of resolving spatial features in the forcing fields down to a length scale of between 400 and 500 km. This may be considered a rather coarse resolution compared with cross-frontal length scales.

(iii) The two surface maps discussed below (Figs. 3 and 8) both show warm frontal and cold frontal lines. There was actually little justification for analysing a warm front on either chart in view of the lack of any obvious discontinuity in surface weather elements across this line, and this feature has therefore been retained only as a means of identifying the principal surface trough axes on the upper level maps.

4. Real case – diagnosis

Surface and 700 mb charts for 0000GMT on 10 November 1975 are shown in Figs. 3 and 4. The surface low is 994 mb and the isallobars indicate significant pressure falls ahead of the system and even larger rises behind. The 700 mb chart shows the cold air associated with the western side of the system.

The Q-vector analysis is given in Fig. 5. The dominant feature is the divergence and

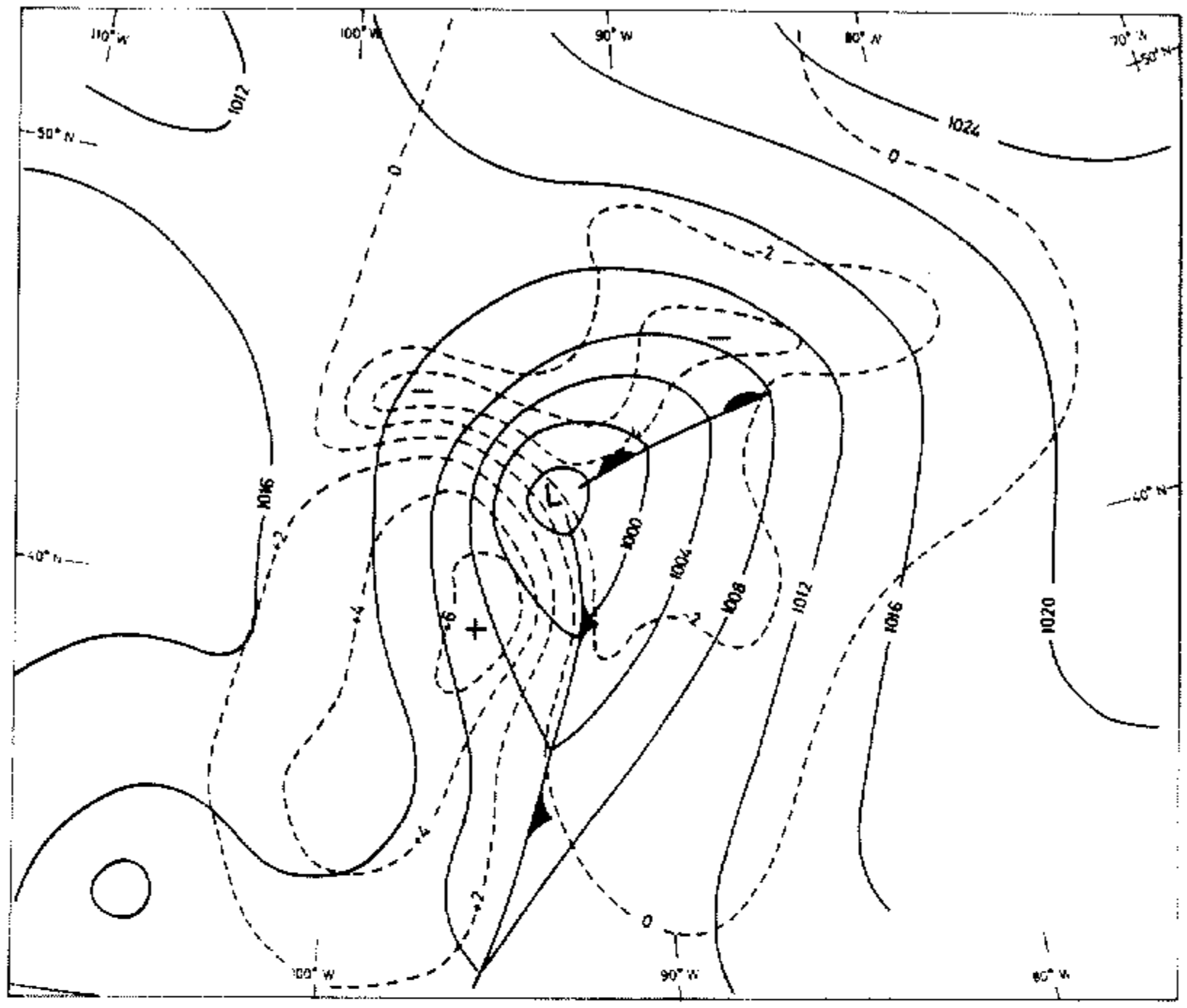

Figure 3. Analysis of surface chart for 0000GMT on 10 November 1975. Isobars are drawn every 4 mb and isallobars every 2 mb $(3h)^{-1}$.

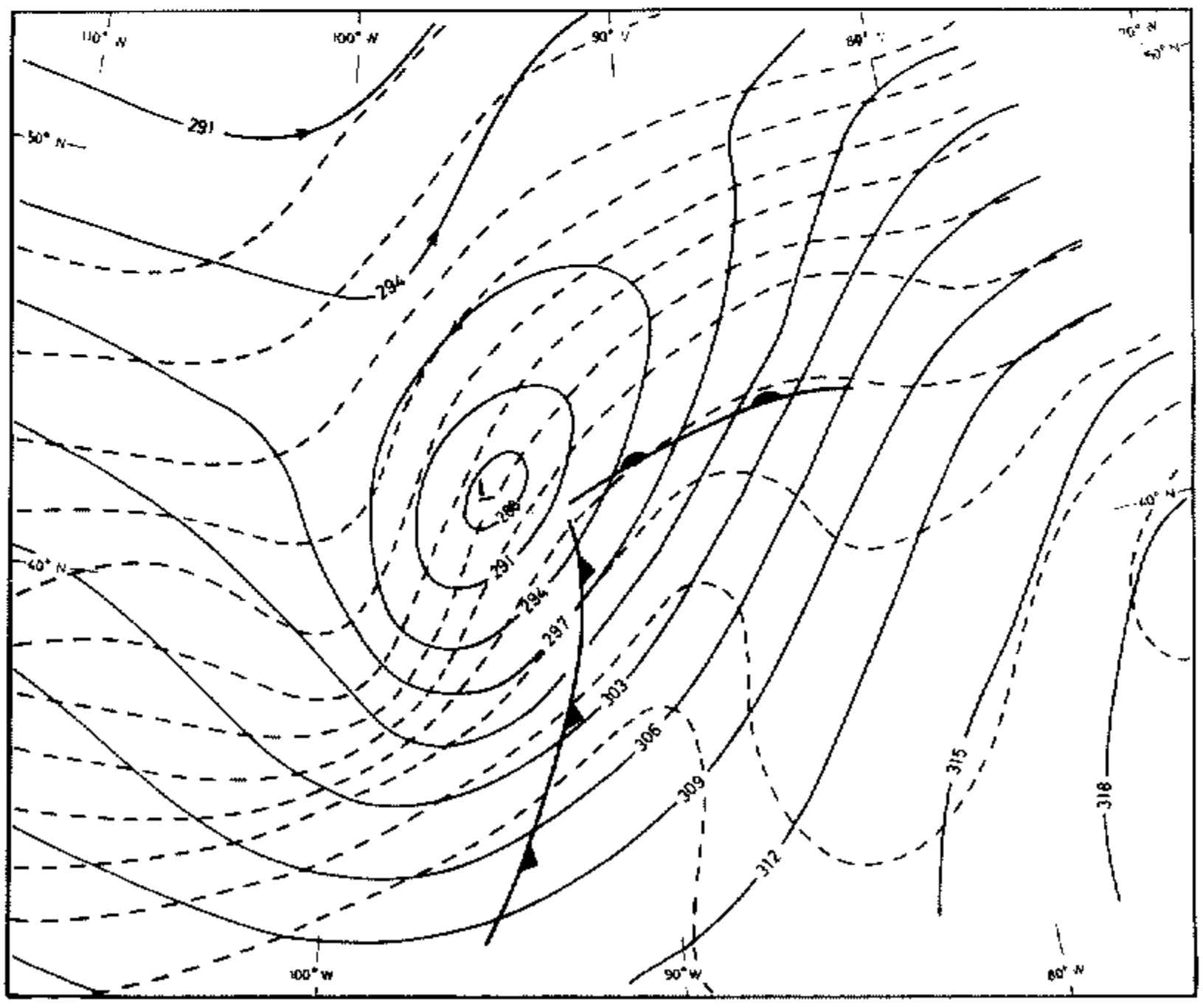

Figure 4. Analysis of 700 mb chart for 0000GMT on 10 November 1975. Height contours are drawn every 30 gpm and temperature contours every 2 K. The surface frontal analysis is indicated.

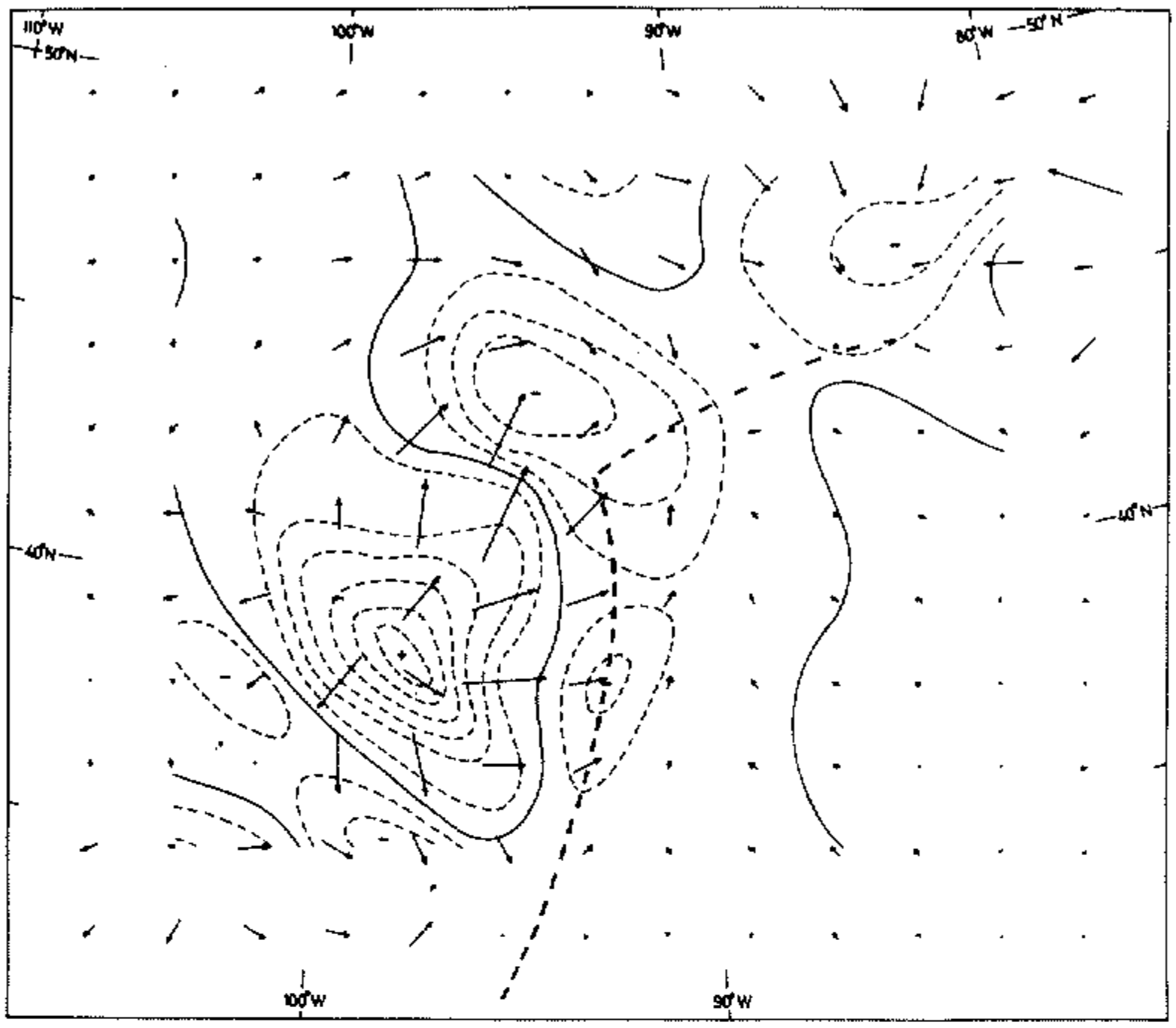

Figure 5. **Q** and $F_Q = (2g/\theta_0)\,\nabla.\mathbf{Q}$ at 700 mb for 0000GMT on 10 November 1975. The length scale for Q is such that the indicated latitudinal distance between grid rows corresponds to approximately 1×10^{-9} $\mathrm{K\,m^{-1}\,s^{-1}}$. Isopleths of F_Q are every $1 \times 10^{-16}\,\mathrm{m^{-1}\,s^{-3}}$ with the zero isopleth being shown as continuous lines. The surface frontal analysis is indicated.

expected descent in the cold air. There is convergence and ascent ahead of the system and to a lesser extent in the cold-frontal region though this is probably underestimated due to the smoothing in the analysis. The crossing of the vectors and the temperature contours in this cold-front region emphasizes the potential frontogenesis there. The warm-frontal region is, however, suggested to be of little importance. All these features are consistent with the isallobaric field, the temperature gradients at 700 mb, and the reported weather.

The forms F_{VT} and F_Q for the forcing term in the omega equation are both exact at the level of quasi-geostrophic theory and thus equal. However, since F_{VT} as given in Eq. (4) contains two separate terms, it is of interest to consider them separately. Figure 6 shows the term proportional to the Laplacian of thermal advection. It tends to dominate the vorticity advection term in this case. However, the cancellation is such that the positive forcing in the cold air in Fig. 6 is a factor of two larger than the resultant. There is also little indication of the cold-frontal circulation.

As was true for the theoretical model depression, the Sutcliffe form for the forcing again captures the main areas of positive and negative forcing but completely misses the cold-front ascent. In Fig. 7 is shown the two-level development theory approximation to the forcing (Eq. (3)). The distribution is very similar to that obtained at 700 mb but the forcing of descent is more than a factor of two smaller.

It is of interest to study the change in the storm in twelve hours. The surface and 700 mb charts for 1200GMT (Figs. 8 and 9) show a centre of about 980 mb with rather larger pressure falls ahead than rises behind, and a well-developed wave in the lower troposphere. This is consistent with the Q-vector analysis in Fig. 10. The convergence and expected ascent ahead of the system are now dominant. The warm-frontal circulation is more apparent than

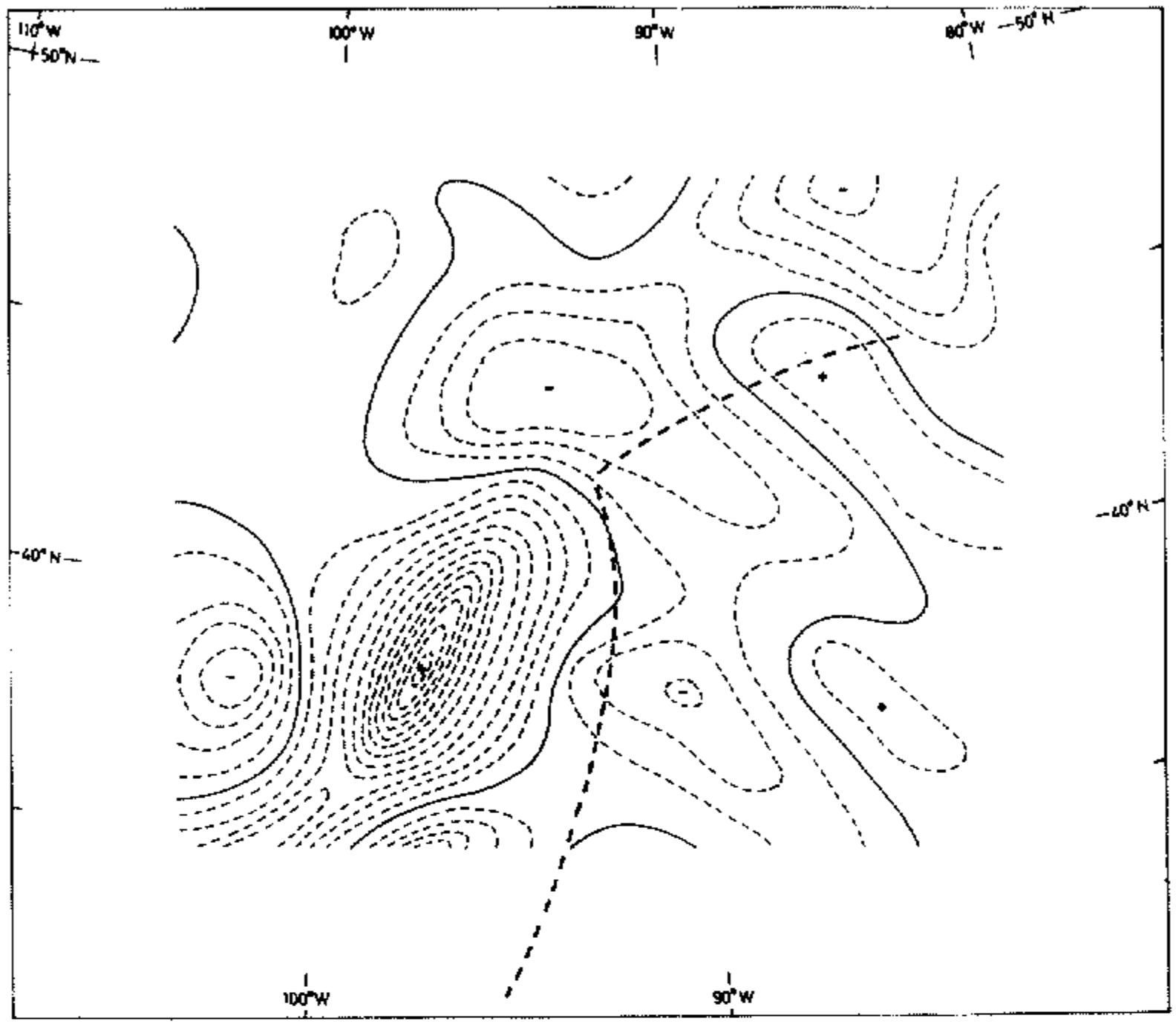

Figure 6. The thermal forcing term (second term in Eq. (4)) at 700 mb for 0000GMT on 10 November 1975. Isopleths are drawn every $1 \times 10^{-16}\,m^{-1}\,s^{-3}$.

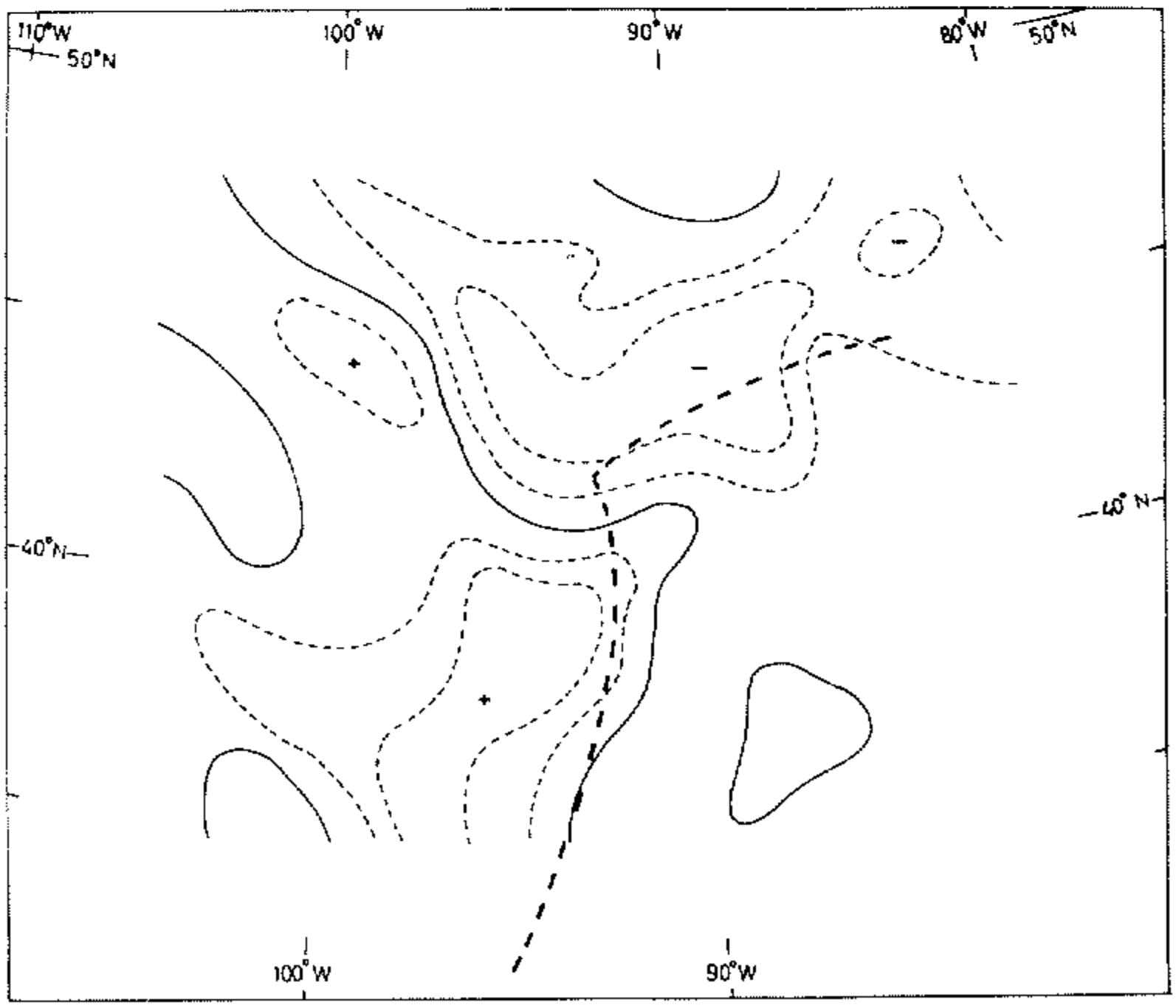

Figure 7. The two-level Sutcliffe form for the forcing (Eq. (3)) based on the 500 mb and 1000 mb levels for 0000GMT on 10 November 1975. Conventions as in Fig. 6.

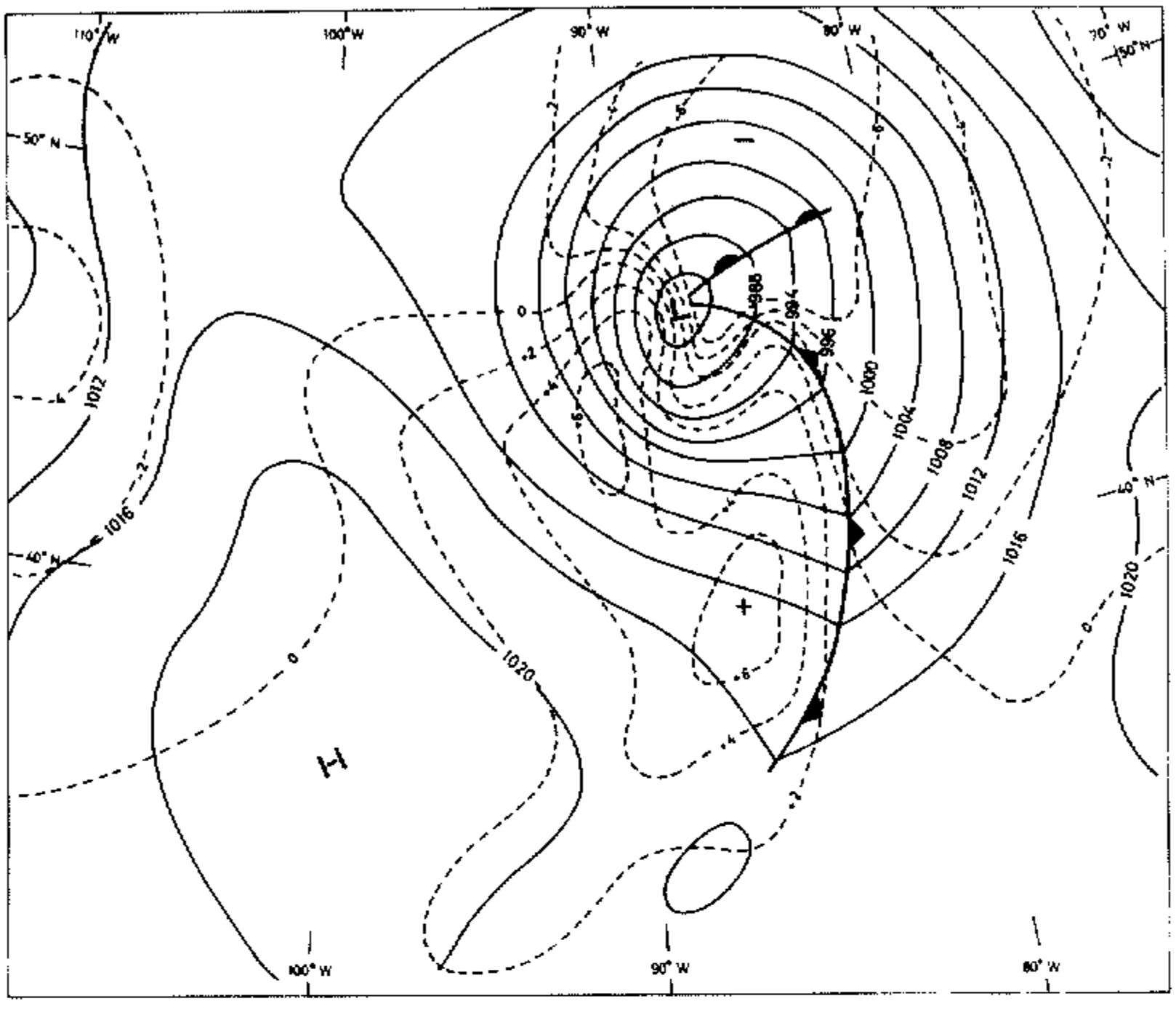

Figure 8. Analysis of surface chart for 1200GMT on 10 November 1975. Conventions as in Fig. 3.

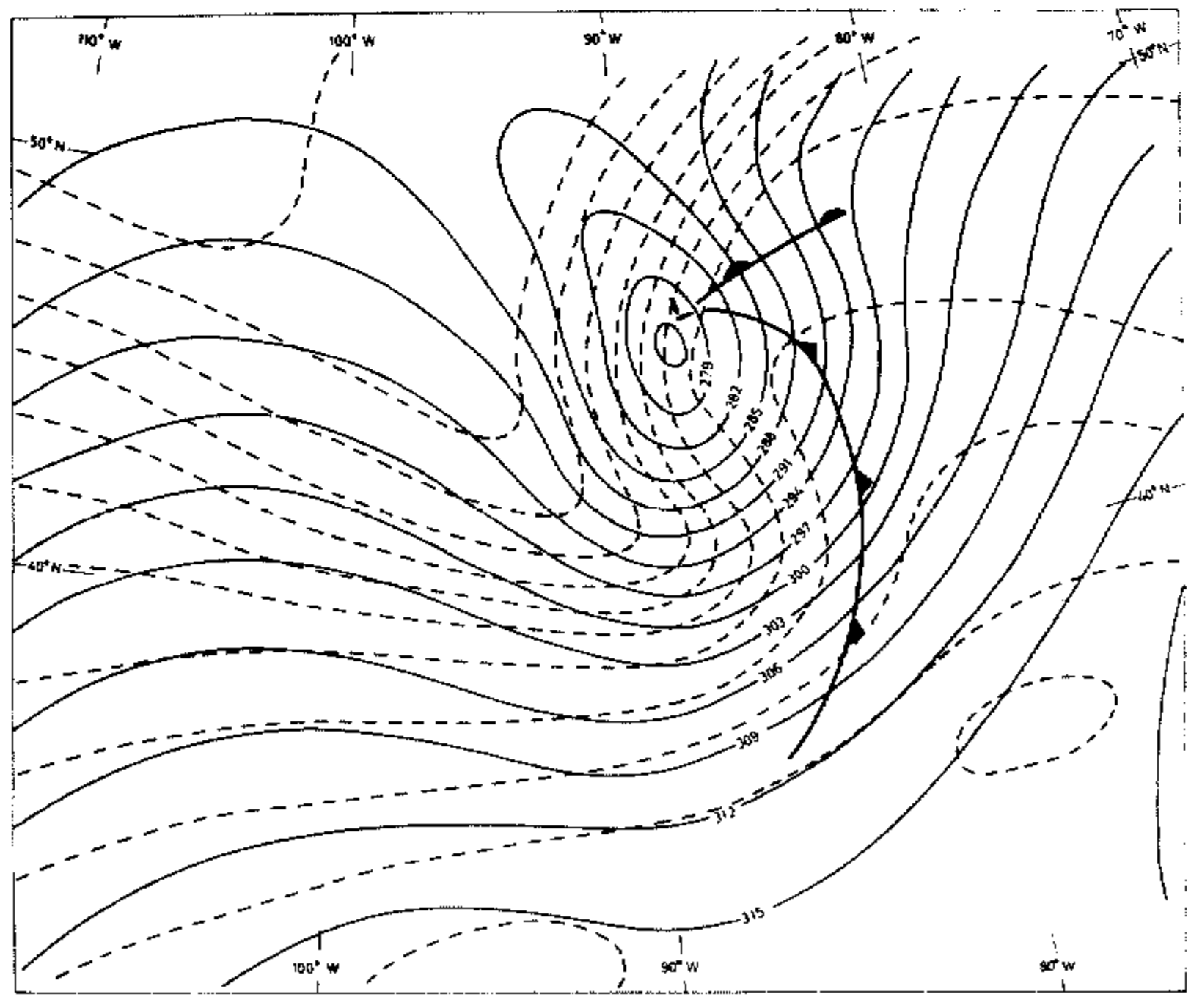

Figure 9. Analysis of 700 mb chart for 1200GMT on 10 November 1975. Conventions as in Fig. 4.

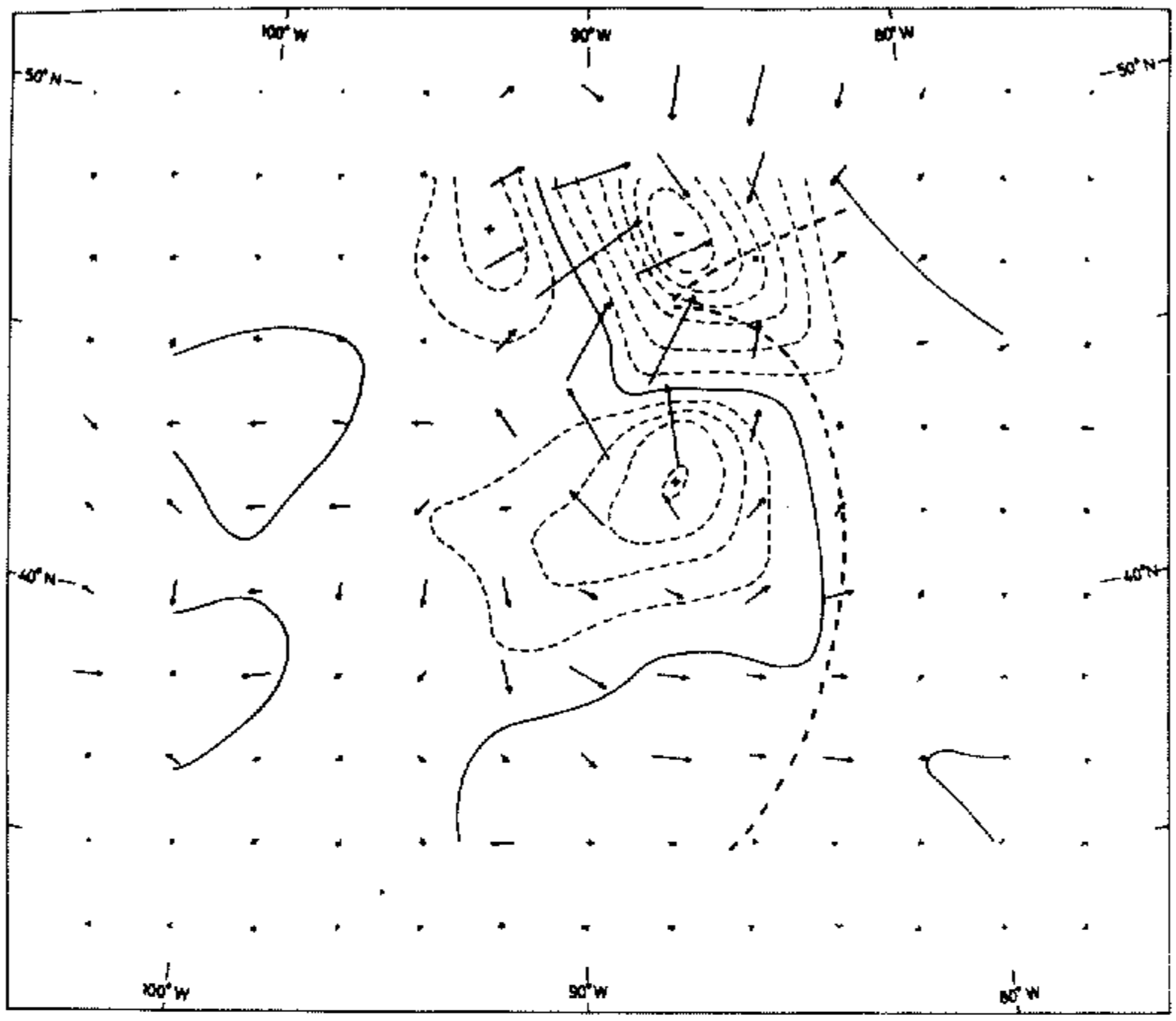

Figure 10. Q and F_Q at 700 mb for 1200GMT on 10 November 1975. Conventions as in Fig. 5 except that the contour interval is now $2\times10^{-16}\,\mathrm{m}^{-1}\,\mathrm{s}^{-3}$ and the scaling for the vectors is halved.

that at the cold front. Thus it appears that the system changed in twelve hours from being dominated by descent in the cold air and the cold frontal circulation to ascent in the warm air and the warm frontal circulation. This behaviour differs from the almost symmetrical picture given by the theoretical baroclinic wave described in section 2 but shows similarities with the downstream development of baroclinic waves discussed in Simmons and Hoskins (1979). There the analysis concentrated on the growth of baroclinic waves in space as well as in time from an initially local perturbation.

5. Conclusion

The vorticity and thermal advection form for the forcing of the omega equation is exact at the level of quasi-geostrophic theory, but because of cancellation problems between two terms involving either a vertical derivative or a horizontal Laplacian this form is not suitable for qualitative reasoning. The Sutcliffe form is the easiest for qualitative argument about system vertical velocities and consequent development. However, the approximations made mean that it is not applicable to regions of large deformation, in particular to frontal regions. The usual two-level approximation loses yet more information on relative intensities of ascent and descent. The Q-vector method is exact and does not suffer from cancellation problems but is not as simple as the Sutcliffe form for qualitative argument, though such argument is possible as was demonstrated in Ω. The plotting of Q-vectors in analysis and forecast charts should, however, be a trivial numerical operation.

It might be asked whether the plotting of vertical velocities, if available, might not be preferable to plotting Q-vectors. Instantaneous vertical velocities from a moist primitive equation model are unreliable in presenting the important patterns of weather. A diagnostic

solution of the omega equation or its semi-geostrophic generalisation could be an alternative. However, a plot of Q-vectors for a mid-tropospheric level shows much more than just the forcing term for these vertical velocity equations. It displays the manner in which temperature gradients are tending to change moving with the fluid. This information includes the usual frontogenesis function. The Q-vectors indicate details of the ageostrophic motion, even the ageostrophic vorticity as shown in Appendix B. Active frontal regions with their cross-frontal circulations are picked out as are regions of frontolysis. The lack of any direct account of diabatic processes, particularly latent heat release, in the form of the omega equation on which the Q-vector analysis is based might be thought to be a drawback. However the effect of previous diabatic processes as reflected by the instantaneous geostrophic fields, is included. It is probable that experience would show that reference to a moisture analysis would indicate those regions where the implied upward motion might be expected to be enhanced due to latent heat release. Finally, it is of some practical importance to note that a field of Q-vectors could be superimposed on standard height and thickness or temperature charts without confusing the overall analysis, whereas another set of contours for vertical velocity would probably require separate display.

Acknowledgment

The authors wish to thank Professor R. P. Pearce for his helpful comments on an early version of this paper.

Appendix A

Sutcliffe's development theory

As well as using the two-level form for F_s given in Eq. (3), Sutcliffe (1947) neglected the first term in Eq. (1) and used the two-level representation of the second term:

$$\frac{f^2}{H}\left(\frac{\partial w}{\partial z}\bigg|_H - \frac{\partial w}{\partial z}\bigg|_0\right) = -\frac{f^2}{H}\left\{(\nabla_h \cdot \mathbf{v})\bigg|_H - (\nabla_h \cdot \mathbf{v})\bigg|_0\right\} \quad . \quad . \quad \text{(A1)}$$

Now the quasi-geostrophic low-level vorticity equation is

$$\left(\frac{\partial}{\partial t} + \mathbf{v}_0 \cdot \nabla\right)\xi_0 = -f(\nabla_h \cdot \mathbf{v}_0) \quad . \quad . \quad . \quad \text{(A2)}$$

Taking $z = H$ to be a level where the divergence of the horizontal wind field is relatively small, Eqs. (1), (3), (A1) and (A2) give

$$\left(\frac{\partial}{\partial t} + \mathbf{v}_0 \cdot \nabla_h\right)\xi_0 = -2\mathbf{v}' \cdot (\nabla_h \xi_0) - \mathbf{v}' \cdot (\nabla_h \xi'),$$

$$\left(\frac{\partial}{\partial t} + (\mathbf{v}_0 + 2\mathbf{v}') \cdot \nabla_h\right)\xi_0 = -\mathbf{v}' \cdot (\nabla_h \xi'). \quad . \quad . \quad \text{(A3)}$$

Sutcliffe thus introduced the idea of the surface pattern being advected with the additional velocity $2\mathbf{v}'$, 'thermal steering', and changing due to the term on the right-hand side, 'thermal development'. It is of interest to note that, for a sinusoidal distribution of w in the horizontal and vertical, the two terms on the left-hand side of Eq. (1) have the same spatial structure. The ratio of the first term to the second is $\alpha = N^2H^2/f^2L^2$ where L and H are typical horizontal and vertical scales and quasi-geostrophic scaling for a baroclinic system suggests that $\alpha \sim 1$. Thus by neglecting the first term, Sutcliffe approximately overestimated

the resulting divergence by a factor for which the best guess is about 2. Thus a better approximation would be that the surface pattern is advected with a velocity $\mathbf{v}_0 + \mathbf{v}'$, the wind at the level of non-divergence, and that the 'thermal development' term in Eq. (A3) should be halved. The β-effect, if included, would imply slower eastward movement. The reduction in development due to the static stability term was discussed in a somewhat similar manner by Sumner (1950).

Appendix B

The relation between Q and the ageostrophic motion

Equation (8) in the x and y directions gives

$$N^2\frac{\partial w}{\partial x} - f^2\frac{\partial u_a}{\partial z} = \frac{2g}{\theta_0}Q_1 \quad . \quad . \quad . \quad \text{(B1)}$$

$$N^2\frac{\partial w}{\partial y} - f^2\frac{\partial v_a}{\partial z} = \frac{2g}{\theta_0}Q_2 \quad . \quad . \quad . \quad \text{(B2)}$$

where $\mathbf{Q} = (Q_1, Q_2)$ is defined in Eq. (5). Adding $\partial/\partial x$ of Eq. (B1) and $\partial/\partial y$ of Eq. (B2) leads to the omega equation which with the scaling in Appendix A may be approximately written

$$(\alpha+1)f^2\nabla_h \cdot \frac{\partial \mathbf{u}_a}{\partial z} = -\frac{2g}{\theta_0}(\nabla_h \cdot \mathbf{Q}). \quad . \quad . \quad \text{(B3)}$$

As pointed out by Leith (1980), subtracting $\partial/\partial x$ of Eq. (B2) from $\partial/\partial y$ of Eq. (B1) gives

$$f^2\mathbf{k} \cdot \left(\nabla \wedge \frac{\partial \mathbf{u}_a}{\partial z}\right) = -\frac{2g}{\theta_0}\{\mathbf{k} \cdot (\nabla \wedge \mathbf{Q})\}. \quad . \quad . \quad \text{(B4)}$$

It is easily shown that this is a version of the non-linear balance equation. Thus the divergence and curl of the vertical shear in the ageostrophic wind are approximately proportional to minus the divergence and curl of **Q**. In the lower troposphere we may expect that the ageostrophic velocities are largest near the surface. Therefore, to a reasonable approximation, the divergence and curl of the low-level ageostrophic wind are proportional to the divergence and curl of **Q**, the constant of proportionality being about a factor of $\alpha + 1 \sim 2$ larger for the curl.

Appendix C

Pressure coordinate equations

In synoptic investigations the use of pressure as the vertical coordinate is frequently most convenient. Since the equations discussed in this paper have not been given in this coordinate system they are briefly presented here.

Using standard notation,

$$\partial\phi/\partial p = -h\theta \quad \text{where } h = (R/p)(p/p_0)^\kappa.$$

The thermal wind relations are $f\partial v_g/\partial p = -h\,\partial\theta/\partial x, f\partial u_g/\partial p = h\,\partial\theta/dy$. **Q** is defined as in

Eq. 5 except that horizontal derivatives are in pressure surfaces. Using the thermal wind relations an alternative form is given by

$$h\mathbf{Q} = \left\{ -f\left(\frac{\partial u_g}{\partial p}\frac{\partial v_g}{\partial x} + \frac{\partial v_g}{\partial p}\frac{\partial v_g}{\partial y}\right), \quad f\left(\frac{\partial u_g}{\partial p}\frac{\partial u_g}{\partial x} + \frac{\partial v_g}{\partial p}\frac{\partial u_g}{\partial y}\right)\right\}$$

It should be noted that **Q** may be evaluated from a knowledge of the horizontal and vertical shears in the wind.

Defining $\sigma = -h\, d\bar{\theta}/dp$, the vertical circulation equation in any direction $\hat{\mathbf{i}}$ may be written (cf. Eq. 8):

$$-\sigma\frac{\partial \omega}{\partial x'} + f^2\frac{\partial u_a'}{\partial p} = 2h(\mathbf{Q}\,.\,\hat{\mathbf{i}}).$$

Combining the circulation equation in two orthogonal directions gives (cf. Eq. 1):

$$-\sigma\nabla_h^2\omega - f^2\frac{\partial^2\omega}{\partial p^2} = F$$

where $$F = F_Q = 2h(\nabla_h\,.\,\mathbf{Q}).$$

The Sutcliffe approximation for F is

$$F_s = -2f\frac{\partial \mathbf{v}_g}{\partial p}.(\nabla_h\xi_g)$$

and the equivalent of Eq. 4 is

$$F_{VT} = -f\frac{\partial}{\partial p}\{\mathbf{v}_g\,.\,(\nabla_h\xi_g)\} - h\nabla_h^2\{\mathbf{v}_g\,.\,(\nabla_h\theta)\}.$$

References

Hoskins, B. J., Draghici, I. and Davies, H. C.	1978	A new look at the ω-equation, *Quart. J. R. Met. Soc.*, **104**, 31–38. (Ω)
Hoskins, B. J. and Heckley, W. A.	1980	Cold and warm fronts in baroclinic waves. Submitted to *Quart. J. R. Met. Soc.*
Hoskins, B. J. and West, N. V.	1979	Baroclinic waves and frontogenesis. Part II: Uniform potential vorticity jet flows – cold and warm fronts, *J. Atmos. Sci.*, **36**, 1663–1680.
Leith, C. E.	1980	Nonlinear normal mode initialization and quasi-geostrophic theory, *Ibid.*, **37**, 958–968.
Simmons, A. J. and Hoskins, B. J.	1979	Downstream and upstream development of unstable baroclinic waves, *Ibid.*, **36**, 1239–1254.
Sumner, E. J.	1950	The significance of vertical stability in synoptic development, *Quart. J. R. Met. Soc.*, **76**, 384–392.
Sutcliffe, R. C.	1947	A contribution to the problem of development, *Ibid.*, **73**, 370–383.
Trenberth, K. E.	1978	On the interpretation of the diagnostic quasi-geostrophic omega equation, *Mon. Weath. Rev.*, **106**, 131–137.